

# UniRecGen: Unifying Multi-View 3D Reconstruction and Generation

ZHISHENG HUANG, Texas A&M University, USA

JIAHAO CHEN, Texas A&M University, USA

CHENG LIN, Macau University of Science and Technology, Macau

CHENYU HU, Xidian University, China

HANZHUO HUANG, ShanghaiTech University, China

ZHENGMING YU, Texas A&M University, USA

MENGFEI LI, Hong Kong University of Science and Technology, Hong Kong

YUHENG LIU, University of California, Irvine, USA

ZEKAI GU, Hong Kong University of Science and Technology, Hong Kong

ZIBO ZHAO, ShanghaiTech University, China

YUAN LIU, Hong Kong University of Science and Technology, Hong Kong

XIN LI, Texas A&M University, USA

WENPING WANG, Texas A&M University, USA

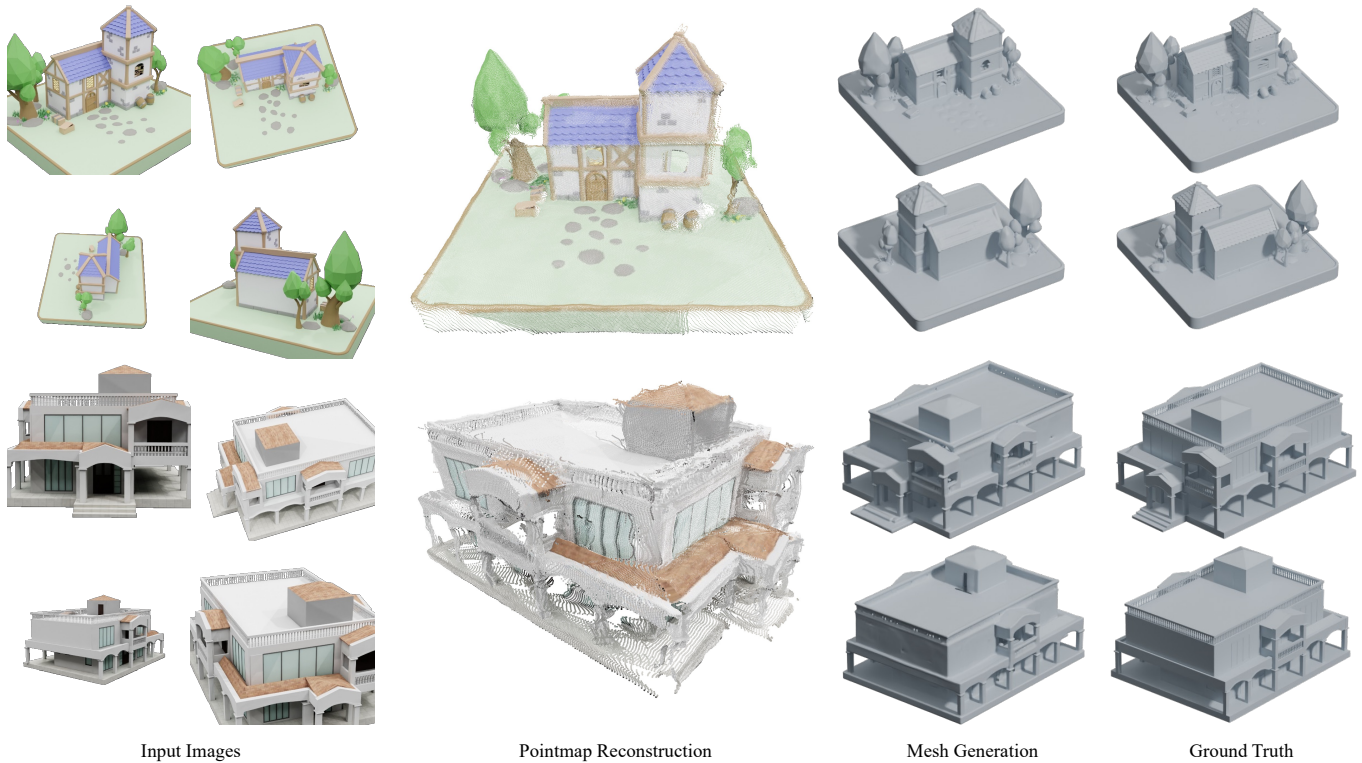


Fig. 1. **UniRecGen enables high-fidelity 3D object reconstruction from sparse, unposed images.** It first establishes a deterministic point-cloud “geometric anchor” within a canonical coordinate system. Guided by this anchor, a generative model synthesizes a detailed mesh that preserves instance-specific structural features while producing plausible geometric completions for unobserved regions, ensuring high alignment with the ground-truth shape.

Sparse-view 3D modeling represents a fundamental tension between reconstruction fidelity and generative plausibility. While feed-forward reconstruction excels in efficiency and input alignment, it often lacks the global priors needed for structural completeness. Conversely, diffusion-based generation provides rich geometric details but struggles with multi-view consistency. We present UniRecGen, a unified framework that integrates these two paradigms into a single cooperative system. To overcome inherent conflicts in coordinate spaces, 3D representations, and training objectives, we align both models within a shared canonical space. We employ disentangled cooperative learning, which maintains stable training while enabling seamless collaboration during inference. Specifically, the reconstruction module is adapted to provide canonical geometric anchors, while the diffusion generator leverages latent-augmented conditioning to refine and complete the geometric structure. Experimental results demonstrate that UniRecGen achieves superior fidelity and robustness, outperforming existing methods in creating complete and consistent 3D models from sparse observations.

CCS Concepts: • **Computing methodologies** → **Shape modeling**.

Additional Key Words and Phrases: 3D Reconstruction, 3D Generation

## 1 Introduction

The quest for high-fidelity 3D object modeling from sparse observations has long been a cornerstone of computer graphics and computer vision. This pursuit has branched into two distinct paradigms: deterministic reconstruction and stochastic generation. The former, typified by recent feed-forward regression models [72], focuses on fidelity by lifting 2D observations into 3D space. However, these methods often suffer from geometric incompleteness and lack the semantic consistency due to their reliance on local features and lack of global structural priors. In contrast, the emergence of 3D diffusion models has introduced powerful object-centric priors, enabling the synthesis of plausible and detailed geometries. Yet, these generative approaches often struggle to remain strictly faithful to the specific fine-grained details provided in the input images, leading to “hallucinations” that deviate from the actual object geometry.

Recently, a prominent trend has emerged seeking to unify these paradigms by aligning the latent spaces of 2D generative models with 3D reconstruction foundations. Notable works such as VIST3A [16] and Gen3R [25] employ model stitching or adapter-based regularization to ensure that the outputs of 2D video diffusion models are inherently decodable by 3D reconstruction systems. While these methods successfully make 2D generation “3D-aware”, they remain fundamentally tethered to the 2D domain. Consequently, they often inherit the “representation gap” and consistency artifacts typical of 2D-to-3D lifting, where the generator must be “policed” to fit a geometric box it does not natively understand.

---

Authors’ Contact Information: Zhisheng Huang, hzs@tamu.edu, Texas A&M University, USA; Jiahao Chen, jiahao.chen@tamu.edu, Texas A&M University, USA; Cheng Lin, chenglin@must.edu.mo, Macau University of Science and Technology, Macau; Chenyu Hu, ch2065@hw.ac.uk, Xidian University, China; Hanzhuo Huang, huanghz2022@shanghaitech.edu.cn, ShanghaiTech University, China; Zhengming Yu, yuzhengming@tamu.edu, Texas A&M University, USA; Mengfei Li, mli@connect.ust.hk, Hong Kong University of Science and Technology, Hong Kong; Yuheng Liu, yuhenl22@uci.edu, University of California, Irvine, USA; Zekai Gu, zekai.gu@u.nus.edu, Hong Kong University of Science and Technology, Hong Kong; Zibo Zhao, zhaozb@shanghaitech.edu.cn, ShanghaiTech University, China; Yuan Liu, yuanly@ust.hk, Hong Kong University of Science and Technology, Hong Kong; Xin Li, xinli@tamu.edu, Texas A&M University, USA; Wenping Wang, wenping@tamu.edu, Texas A&M University, USA.

---

2026. ACM 1557-7368/2026/4-ART  
<https://doi.org/10.1145/nnnnnnn.nnnnnnn>

ACM Trans. Graph., Vol. 1, No. 1, Article . Publication date: April 2026.

In this paper, we propose a departure from alignment-based lifting in favor of native 3D unification. We argue that 3D reconstruction and 3D generation are not competing methodologies, but inherently complementary dimensions of the same 3D inference problem.

Despite the conceptual elegance of this unification, achieving synergy between these two systems presents two fundamental technical challenges: The first challenge is *Disparate Learning Dynamics*. Reconstruction models rely on deterministic regression, while diffusion models operate through stochastic iterative denoising. A naive joint training of these different objectives to interchange information between both sides leads to slow convergence and prohibitive computational overhead, as each module must adapt to the fluctuating and noisy outputs of the other. The second challenge is *Representation and Coordinate Incompatibility*: Feed-forward reconstruction typically operates in camera-relative spaces using explicit geometric features, whereas diffusion-based generation is usually performed in a compact latent space where the latent features are mapped to and interpreted within a canonical, object-centric coordinate system. This misalignment prevents effective information flow and structural collaboration between the two modules.

To address disparate learning dynamics, we adopt an isolated modular design for a holistic 3D system. In this framework, the reconstruction model is trained first to provide a stable geometric anchor that preserves fidelity to the input observations. The generation model is then trained as a prior-driven refiner to recover unobserved regions and synthesize fine-grained details. This decomposition follows the structure of the problem: the system should first ground itself in the visible sparse evidence to establish a factual geometric foundation, and then leverage global shape priors to infer missing structures. As a result, the outputs remain faithful to the evidence while achieving complete, high-fidelity synthesis. Beyond performance, the modular design offers long-term utility: sub-modules can be swapped as stronger models emerge, intermediate outputs enable interpretable monitoring, and external priors can be injected without retraining the entire system.

To resolve the second challenge of representation and coordinate incompatibility, we establish a shared canonical 3D modeling space that serves as a unified structural bridge. Through proposed branch repurposing strategy, we transform the reconstruction model’s native coordinate system into this canonical space, ensuring its outputs are natively interpretable by the generative framework. This shared foundation enables a latent-augmented multi-view conditioning strategy, where the reconstruction results—specifically pointmaps and intermediate features—serve as a robust geometric scaffold to guide the 3D diffusion process. The key insight behind this design is that while point-based signals provide essential constraints for 3D spatial reasoning, they are discontinuous or noisy in capturing fine-grained details. We therefore incorporate multi-view DINO tokens to maintain the high-fidelity synthesis capabilities of the base model. To ensure spatial consistency across these views, geometric tokens from the reconstruction model act as structural anchors, allowing the generative module to precisely localize and distinguish semantic information within the established 3D foundation.

Our main contributions are summarized as follows:

- We introduce UniRecGen, a unified framework that integrates both 3D reconstruction and generation for 3D object shape modeling from unposed multi-view images.
- We propose to adopt a modular design to avoid disparate learning dynamics during the unification.
- We establish a shared canonical 3D space by leveraging the branch repurposing and the latent-augmented multi-view conditioning strategy to address representation and coordinate incompatibility during unification.
- Experimental results demonstrate that our methods significantly outperform SOTA methods in both multi-view consistency and mesh generation quality.

## 2 Related Work

### 2.1 3D Generation

The field of 3D content generation has rapidly shifted from costly per-scene optimization to efficient, scalable generative frameworks capable of producing high-quality assets in seconds. Initial efforts leveraged Generative Adversarial Networks (GANs) [17] to learn distributions over various 3D representations [1, 15, 80], but these struggled to scale to diverse and complex shapes. The introduction of diffusion models [23, 60] marked a turning point, enabling higher-quality generation across multiple 3D representations including point clouds [46, 49, 69], voxel grids [26, 48], neural radiance fields [4, 47], and signed distance functions [52, 100]. More recently, 3D Gaussian Splatting (3DGS) [30] has emerged as an efficient representation inspiring new generative models [21, 64, 93].

To reduce the cost of high-dimensional 3D generation, recent methods adopt latent diffusion approaches [54] that compresses 3D data into compact latent spaces for efficient modeling. Current native 3D generative methods broadly fall into three main categories: vector set-based methods [9, 24, 27, 31, 32, 35, 36, 41, 66, 82, 87, 94, 96, 98, 99], sparse voxel-based methods [22, 37, 83, 84, 91], and autoregressive mesh generation [5, 7, 8, 19, 59, 65, 77, 79, 97].

An alternative paradigm leverages pretrained 2D diffusion models via score distillation sampling [53, 78, 81], but it relies on costly test-time optimization and often yields inconsistent geometry [67, 78]. Multi-view diffusion models [10, 34, 38, 39, 42–44, 57, 58, 62, 70, 85, 88] generate consistent views for 3D reconstruction but typically produce less accurate geometry than native 3D methods.

Despite rapid progress in 3D generation, recovering high-fidelity 3D assets from multiple unposed RGB images remains underexplored, as it requires fine geometry and strong multi-view consistency without known camera poses. Closest to our setting, PF-LRM [73] addresses pose-free reconstruction but is limited by a Tri-plane NeRF representation, while the concurrent ReconViaGen [2] explores reconstruction via generative priors with a multi-stage pipeline. In contrast, we canonicalize VGGT predictions into an object-centric space and directly condition Hunyuan3D-Omni on latent geometry and dense multi-view appearance features, enabling a simpler and more interpretable pipeline for unposed inputs.

### 2.2 Multi-View 3D Reconstruction

Traditional 3D reconstruction typically relies on Structure-from-Motion [55] and Multi-View Stereo [56] to recover geometry via

photometric consistency and triangulation. While learning-based MVS methods [18, 71, 89, 90] have improved efficiency through deep cost volume regularization, they remain sensitive to camera pose accuracy and often struggle with sparse inputs [63]. Alternatively, Neural Radiance Fields [47] enable high-quality synthesis via differentiable rendering, yet they frequently suffer from overfitting under sparse views and require costly per-scene optimization despite various regularization strategies [50, 74, 92].

The advent of 3DGS [30] has inspired feed-forward architectures that directly regress Gaussian parameters from sparse multi-view features [3, 29, 68, 95], achieving impressive speed and generalization. However, these approaches fundamentally rely on local geometric features and lack strong cross-view priors. Consequently, they often produce incomplete reconstructions with visible artifacts in occluded regions, particularly when view overlap is minimal.

A significant bottleneck remains the dependency on external pose estimation. While some pose-free methods attempt to jointly optimize camera parameters and geometry [13, 14, 40], they are often prone to local minima. Recent stereo foundation models, such as DUS<sub>t</sub>3R [75], MAS<sub>t</sub>3R [33], and VGGT [72], address this by predicting aligned point maps via dense correspondence. Although these models enable robust pose-free reconstruction, they typically yield point clouds that lack surface topology or completeness.

In contrast to methods relying solely on per-view geometry, our work integrates feed-forward reconstruction with generative 3D priors learned from large-scale data. By adapting VGGT to predict in a canonical space and conditioning diffusion-based generation on its geometric features, we leverage both precise stereo correspondence and learned shape priors to produce complete, high-fidelity 3D objects from arbitrary unposed sparse views.

## 3 Method

Given an arbitrary number of unposed input images of an object, our method aims to recover high-fidelity 3D shape by unifying feed-forward multi-view geometry estimation and controllable 3D generation. A fundamental challenge is that feed-forward geometry foundations typically predict camera-centric, view-dependent outputs that are not directly compatible with object-centric generative priors; meanwhile, 3D generators assume canonical object space and require reliable geometric guidance to remain faithful to the input views. To bridge this gap, we propose a two-stage modular pipeline. First, we canonicalize the feed-forward geometry predictions via a branch-repurposing strategy, producing generation-compatible canonical point maps and a refined canonical point cloud through similarity alignment (Sec. 3.2). Second, we train a controllable 3D generator with latent-augmented multi-view conditioning, combining dense image tokens with geometry and camera embeddings to inject multi-view geometric context while retaining strong appearance priors (Sec. 3.3). This modular design preserves pretrained priors, supports model interchangeability, and enables effective geometry-guided generation. An overview of our method is presented in Fig. 2.

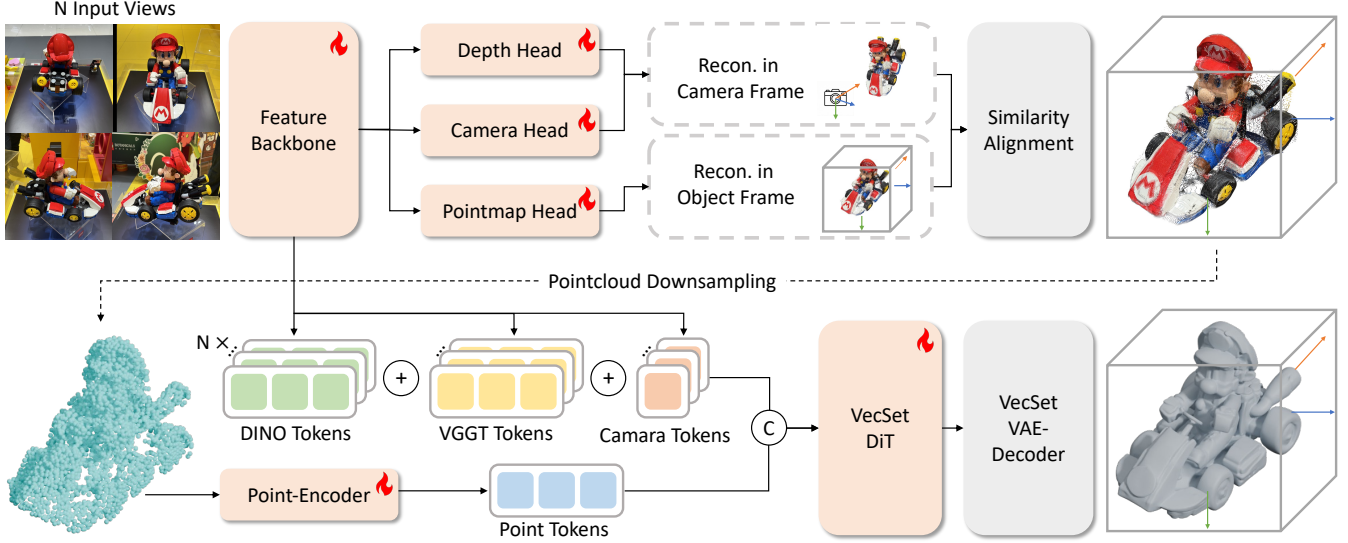


Fig. 2. **Overview of our method.** Given  $N$  unposed input views, we first canonicalize feed-forward multi-view geometry predictions via branch repurposing and similarity alignment to obtain a canonical point cloud (top). We then train a controllable 3D generator conditioned on this point cloud together with multi-view image features, geometry latents, and camera embeddings to synthesize a high-fidelity mesh (bottom).

### 3.1 Preliminaries

**Feed-Forward 3D Reconstruction.** Recent advancements in 3D vision have seen a significant shift from traditional optimization-based pipelines toward unified feedforward architectures. Foundational models such as DUST3R [75] and MAST3R [33] pioneered this transition by formulating 3D reconstruction as a dense pointmap regression task, enabling pose-free reconstruction from image pairs. While powerful, extending these pairwise methods to large-scale multiview scenarios often requires expensive global alignment or post-processing. To overcome these constraints, more recent feed-forward geometry models such as VGGT [72], along with contemporaneous and subsequent works including Fast3R [86] and  $\pi^3$  [76], have introduced a more scalable paradigm. These models leverage large-scale Transformers to jointly regress camera parameters and scene geometry across an arbitrary number of views in a single pass. We adopt this scalable feedforward multiview representation as our foundation, choosing VGGT as a representative instantiation due to its inherent efficiency and ability to maintain global geometric consistency without iterative optimization. Given multi-view images  $\{\mathbf{I}_i \in \mathbb{R}^{H \times W \times 3}\}_{i=1}^N$ , VGGT first extracts their spatial features  $\mathbf{F}_i^D \in \mathbb{R}^{K \times C}$  via DINO [51] and concatenates them with additional camera tokens  $\mathbf{t}_i^{\text{cam}} \in \mathbb{R}^{1 \times C}$ , where  $K$  is the spatial token number for each image and  $C$  is the feature dimension. These tokens are later processed through a large transformer to obtain VGGT tokens  $\mathbf{F}_i^V \in \mathbb{R}^{K \times C}$  and refined camera tokens  $\hat{\mathbf{t}}_i^{\text{cam}} \in \mathbb{R}^{1 \times C}$ . For different tasks, VGGT adopts three prediction heads: (1) the *Camera head* that maps camera tokens  $\hat{\mathbf{t}}_i^{\text{cam}}$  to camera parameters  $\mathbf{g}_i^{\text{ref}} \in \mathbb{R}^9$  in the first camera’s reference frame; (2) the *Depth head* that maps VGGT tokens  $\mathbf{F}_i^V$  to pixel-wise depth maps  $\mathbf{D}_i^{\text{ref}} \in \mathbb{R}^{H \times W}$ ; and (3) the *Point head* that maps VGGT tokens  $\mathbf{F}_i^V$  to viewpoint-invariant point maps  $\mathbf{P}_i^{\text{ref}} \in \mathbb{R}^{H \times W \times 3}$  in the reference frame. The entire model is optimized end-to-end using multi-task regression losses as follows:

$$\mathcal{L} = \mathcal{L}_{\text{camera}} + \mathcal{L}_{\text{depth}} + \mathcal{L}_{\text{pmap}} + \lambda \mathcal{L}_{\text{track}}. \quad (1)$$

**Controllable 3D Generation.** 3D generation has largely converged on a latent generative paradigm, where high-dimensional 3D geometry is first compressed into a structured latent space and then synthesized via conditional diffusion (or flow-based) models. This design substantially reduces the computational burden of modeling directly in 3D while enabling flexible control through multi-modal conditioning. While our framework is designed to be compatible with various 3D generative backends, we utilize Hunyuan3D-Omni [28] as a representative instantiation. By leveraging its multi-modal control encoder, we can directly incorporate geometric guidance while bypassing the substantial overhead of training a conditioned generative prior from scratch. Hunyuan3D-Omni operates by first mapping 3D geometry into a structured latent space, followed by a diffusion process to synthesize novel shapes. Given a surface-sampled point set  $\mathcal{S} \in \mathbb{R}^{N \times 6}$  that concatenates 3D coordinates with surface normals, the Transformer-based encoder maps  $\mathcal{S}$  into a sequence of latent tokens  $\mathbf{Z} \in \mathbb{R}^{L \times C}$ . These latent tokens are subsequently processed by a diffusion transformer under a multi-modal conditioning signal  $\text{cond} = [\mathbf{F}^D, \beta]$ , where  $\mathbf{F}^D$  represents DINO-extracted image features and  $\beta$  denotes the embedding produced by the unified control encoder for point-cloud, voxel, bounding-box, and skeletal conditions. To produce the final output, the denoised representation is decoded into a signed distance field  $F_{\text{sdf}}$ , from which high-quality triangular meshes are extracted via marching cubes [45]. The framework is optimized end-to-end using a flow-matching objective:

$$\mathcal{L} = \mathbb{E}_{t, x_0, x_1, \text{cond}} \|u_{\theta}(x_t, t, \text{cond}) - (x_1 - x_0)\|_2^2, \quad (2)$$

where  $x_0$  is Gaussian noise,  $x_1$  is the latent sample, and  $x_t = (1 - t)x_0 + tx_1$  describes the trajectory under  $t \sim \mathcal{U}(0, 1)$ .

**3.2 Generation-compatible Feed-Forward Reconstruction**  
Feed-forward 3D reconstruction methods [72, 76, 86] demonstrate robust open-world generalization by leveraging massive, diverse

training corpora. A shared characteristic is their multi-head prediction architecture. In the case of VGGT, this involves a combination of relative camera poses ( $\mathbf{g}_i^{\text{ref}}$ ), per-view depth maps ( $\mathbf{D}_i^{\text{ref}}$ ), and global point maps ( $\mathbf{P}_i^{\text{ref}}$ ). To maintain scene-agnostic flexibility, these architectures typically represent geometry within a relative reference frame, often defined by the coordinate system of the primary input camera. Conversely, 3D generative frameworks model shapes in a canonical, object-centered space to ensure consistent orientation, scale, and topological integrity. This mismatch makes foundation reconstructions difficult to directly guide generation pipelines: their outputs are camera-centric and thus not directly compatible with canonical-space shape priors. We address this by canonicalizing feed-forward reconstruction prediction.

**Design Space Exploration.** We explore three approaches to achieve canonical space prediction:

- *Direct supervision transferring:* Directly supervise all heads in canonical space, but this causes degradation of pretrained 3D priors.
- *Explicit transformation prediction:* Add dedicated tokens and heads to predict reference-to-canonical transformation, but weak gradient signals lead to slow convergence and poor performance.
- *Branch repurposing (ours):* Repurpose only the point map head to output  $\mathbf{P}_i^{\text{can}}$  in canonical space, while keeping  $\mathbf{g}_i^{\text{ref}}$  and  $\mathbf{D}_i^{\text{ref}}$  in the reference frame.

**Our Approach.** We adopt branch repurposing based on three key insights: (1) Maintaining  $\mathbf{g}_i^{\text{ref}}$  and  $\mathbf{D}_i^{\text{ref}}$  in the reference frame provides strong regularization preserving VGGT’s learned priors. (2) Supervising only  $\mathbf{P}_i^{\text{can}}$  in canonical space provides dense gradient signals for effective adaptation. (3) We can transform the more accurate depth predictions to canonical space via similarity alignment with  $\mathbf{P}_i^{\text{can}}$ , obtaining better geometry than using  $\mathbf{P}_i^{\text{can}}$  alone. Specifically, we align depth-derived 3D points (from  $\mathbf{g}_i^{\text{ref}}$  and  $\mathbf{D}_i^{\text{ref}}$ ) with predicted canonical points  $\mathbf{P}_i^{\text{can}}$ . We apply two-stage sampling: uniform sampling yields  $4M$  points, then Farthest Point Sampling (FPS) selects  $M$  spatially diverse correspondences.

The similarity transformation  $\mathbf{T} \in \text{Sim}(3)$  is computed via weighted Procrustes analysis:

$$\mathbf{T} = \underset{\mathbf{T} \in \text{Sim}(3)}{\text{argmin}} \sum_{j=1}^M w_j \|\mathbf{P}_j^{\text{can}} - \mathbf{T}(\mathbf{D}_j^{\text{ref}})\|^2, \quad (3)$$

where  $w_j$  denotes confidence weights,  $\mathbf{D}_j^{\text{ref}}$  represents the  $j$ -th depth-derived 3D point, and  $\text{Sim}(3)$  encompasses rotation, translation, and uniform scaling.

### 3.3 Reconstruction-guided Controllable Generation

Having obtained a canonicalized 3D reconstruction from a feed-forward model, we next leverage these results as conditioning signals for controllable 3D generation. We adopt Hunyuan3D-Omni (see Section 3.1), which supports point-cloud conditioning to guide shape synthesis. This design naturally allows us to use the generation-compatible pointmap as direct geometric control. However, without further training, we observe that the generation model fails to deliver high-fidelity 3D object generation due to the following: (1)

VGGT 3D reconstruction features outliers and noise, this kind of point cloud conditioning is not seen by the Hunyuan3D-Omni generation model during training. (2) Point cloud conditioning could only provide limited geometry details as it doesn’t contain continuous surface information. (3) Hunyuan3D-Omni is limited to single view conditioning, failing to leverage multi-view image information.

To this end, we further train the Hunyuan3D-Omni generation model to fully leverage the 3D object reconstruction results. Specifically, we modify the model to condition on both point-cloud and multi-view images. We keep the  $\beta$  (See Section 3.1) unchanged, while modifying the joint conditioning to

$$\text{cond} = [\mathbf{F}_1^{MV}, \mathbf{F}_2^{MV}, \dots, \mathbf{F}_N^{MV}, \beta], \quad (4)$$

where  $\mathbf{F}_i^{MV}$  denotes the multi-view conditioned features for the  $i$ -th frame. This simple yet effective approach allows us to fully exploit the strengths of the base Hunyuan3D-Omni model by retaining the original point cloud conditioning pathway.

**Design Space Exploration.** We investigate two distinct paradigms for integrating multi-view geometric conditioning into the generative pipeline:

- *Point-Guided Feature Sampling:* In this configuration, the conditioning points  $\mathbf{P}^c$  (downsampled from the initial VGGT reconstruction) are used to index a corresponding subset of multi-view DINO tokens. This aims to strike a balance between image-derived semantic signals and explicit geometric constraints. These features are further augmented with 3D positional encodings of  $\mathbf{P}_i^c$  to provide spatial grounding:

$$\mathbf{F}_i^{MV} = \mathcal{S}(\mathbf{F}_i^D, \mathbf{P}^c) + \text{MLP}(\text{PE}(\mathbf{P}^c)), \quad (5)$$

where  $\mathcal{S}(\cdot, \mathbf{P}^c)$  denotes the spatial sampling operator indexed by points  $\mathbf{P}^c$ .

- *Latent-Augmented View Conditioning (Ours):* Rather than sparsifying the feature space, we enrich the full set of DINO tokens  $\mathbf{F}_i^D$  by injecting view-dependent geometric context. We project VGGT latent tokens and camera tokens via learnable MLPs to serve as geometric embeddings:

$$\mathbf{F}_i^{MV} = \mathbf{F}_i^D + \text{MLP}_{\text{view}}(\mathbf{F}_i^V) + \text{MLP}_{\text{cam}}(\hat{\mathbf{t}}_i^{\text{cam}}). \quad (6)$$

**Our Approach.** We adopt the latent-augmented approach based on two key insights: (1) Hunyuan3D-Omni’s synthesis quality relies on dense semantic priors within DINO tokens rather than sparse geometric constraints, which stems from the fact that Hunyuan3D-Omni is built upon Hunyuan3D 2.1, an image-to-3D generation model. Besides, images inherently contain richer structural information than point clouds. (2) VGGT tokens  $\mathbf{F}_i^V$  represent a continuous, learned geometric manifold with global structural coherence and multi-scale spatial context, which enables the diffusion model to better integrate multi-view information.

## 4 Experiments

### 4.1 Implementation Details

**Data Preparation.** Our model is trained on a curated subset of Objaverse-XL [11], a large-scale repository of over 10 million 3D objects. Following the filtering pipeline in TRELIS [84], we select models based on aesthetic scores and further exclude objects with

Table 1. **Quantitative Results for 3D Object Reconstruction.** We report geometric metrics across the Toys4K and GSO datasets. Our framework consistently outperforms existing generative and reconstruction-based methods across all metrics.

Dataset	Method	Chamfer- $L_2$ ↓	Prec. ↑	Rec. ↑	F-Score ↑	Normal ↑	IoU ↑
Toys4K	LucidFusion [20]	0.1333	0.2143	0.1378	0.1471	0.6240	0.1035
	Hunyuanyuan3D-MV [98]	0.0513	0.4930	0.4305	0.4540	0.8124	0.6311
	TRELLIS-M [84]	0.0343	0.5952	0.5600	0.5674	0.8309	0.6318
	TRELLIS-S [84]	0.0309	0.5762	0.5430	0.5525	0.8324	0.6583
	SAM 3D [6]	0.0354	0.5416	<u>0.6575</u>	0.5711	0.8218	0.6061
	ReconViaGen [2]	<u>0.0281</u>	<u>0.6224</u>	0.6086	<u>0.6105</u>	<u>0.8543</u>	<u>0.7229</u>
	<b>Ours</b>	<b>0.0175</b>	<b>0.7622</b>	<b>0.7834</b>	<b>0.7695</b>	<b>0.8785</b>	<b>0.8030</b>
GSO	LucidFusion [20]	0.1203	0.2004	0.1648	0.1650	0.6421	0.1317
	Hunyuanyuan3D-MV [98]	0.0667	0.4060	0.3680	0.3781	0.7897	0.5980
	TRELLIS-M [84]	0.0318	0.5071	0.4863	0.4918	0.8482	0.6489
	TRELLIS-S [84]	0.0391	0.4771	0.4526	0.4605	0.8302	0.6486
	SAM 3D [6]	0.0296	0.5311	<u>0.7044</u>	0.5872	0.8535	0.6339
	ReconViaGen [2]	<u>0.0290</u>	<u>0.6167</u>	0.6149	<u>0.6069</u>	<u>0.8751</u>	<u>0.6918</u>
	<b>Ours</b>	<b>0.0192</b>	<b>0.7322</b>	<b>0.7540</b>	<b>0.7384</b>	<b>0.9023</b>	<b>0.8155</b>

transparent materials, resulting in a final training set of 40K high-quality 3D models. For each object, we render 50 viewpoints from randomly sampled camera poses using Blender to obtain multi-view RGB and depth images. For evaluation, we select 100 objects from each of two widely-used benchmarks: Google Scanned Objects (GSO) [12], which consists of high-quality scanned household items with diverse geometries and realistic textures, and Toys4k [61], a collection of high-quality 3D toy meshes across different categories. For each object, we synthesize 24 multi-view RGB images across a diverse range of field-of-views, elevations, and azimuths. To simulate realistic conditions, we apply random perturbations to the camera translations. From this set of 24 views, we randomly select a 4-view subset as input to our model, allowing us to evaluate its performance in a challenging sparse-view reconstruction setting.

**Network Training.** We train our framework in two stages for stability and efficiency. In Stage I, we adapt the feed-forward multi-view reconstruction module to produce generation-compatible canonical predictions. We follow the standard training recipe of [72] with two modifications: (1) we omit the tracking loss to simplify the objective and improve throughput, and (2) for each iteration, we randomly sample 4 views from the 50 rendered viewpoints per object. Training runs for 80K steps with a peak learning rate of  $1 \times 10^{-5}$  and a 1K-step linear warmup, using 4 NVIDIA H800 GPUs with a total batch size of 32 (about 5 days). In Stage II, we freeze the reconstruction module and train the 3D generator using the diffusion loss in Eq. (2). We sample ground-truth point clouds on-the-fly; to reduce supervision ambiguity caused by residual misalignment between ground truth and the predicted canonical geometry, we align the ground-truth point cloud to the predicted geometry with a similarity transform before encoding it into the latent space. The generator is trained for 80K steps with a peak learning rate of  $1 \times 10^{-5}$  and a 1K-step warmup on 4 NVIDIA H800 GPUs with a batch size of 32 over 8 days.

**Evaluation Metrics.** We evaluate camera poses using *Absolute Trajectory Error* (ATE) and *Relative Pose Error* (RPE), reporting both translation ( $RPE_t$ ) and rotation ( $RPE_r$ ) components. To assess depth

Table 2. **Quantitative Comparison of Camera Pose Estimation.** We evaluate Absolute Trajectory Error (ATE) and Relative Pose Error (RPE) for translation ( $t$ ) and rotation ( $r$ ) on the GSO and Toys4k benchmarks.

Method	GSO			Toys4k		
	ATE ↓	$RPE_t$ ↓	$RPE_r$ ↓	ATE ↓	$RPE_t$ ↓	$RPE_r$ ↓
VGGT [72]	0.0799	0.1856	8.18	0.1209	0.2931	19.14
ReconViaGen [2]	<u>0.0190</u>	<u>0.0443</u>	<b>2.12</b>	<u>0.0425</u>	<u>0.1099</u>	<u>8.53</u>
<b>Ours</b>	<b>0.0151</b>	<b>0.0338</b>	<u>2.16</u>	<b>0.0255</b>	<b>0.0637</b>	<b>3.67</b>

accuracy, we employ *Absolute Relative Error* (Abs Rel), which measures the mean percentage error relative to ground truth, and *Root Mean Square Error* (RMSE), which penalizes larger depth outliers to reflect global coordinate alignment. To comprehensively evaluate the geometric quality of the reconstructed meshes, we employ several standard 3D metrics: *Chamfer- $L_2$  Distance* (CD) measures the average squared distance between sampled points on the reconstructed and ground-truth surfaces; *Precision* and *Recall* calculate the percentage of points within a distance threshold ( $d < 0.01$ ) of each other; *F-Score* provides a balanced assessment of surface coverage and accuracy; *Normal Consistency* (NC) evaluates the average cosine similarity between surface normals to reflect orientation accuracy; and *Voxel IoU* measures volumetric overlap on a  $128^3$  grid.

## 4.2 Comparison with State-of-the-Art Methods

**Multi-view Camera Pose and Depth Estimation.** We first evaluate our method on multi-view camera pose and depth estimation using the GSO and Toys4k datasets. We benchmark our model against the original VGGT baseline [72] and ReconViaGen [2]. We choose ReconViaGen for comparison as it represents the most relevant contemporary work to our approach; specifically, it is also built upon the VGGT architecture and leverages generative models to enhance 3D object reconstruction. The quantitative results are detailed in Table 2 and Table 3. While both our method and ReconViaGen significantly outperform the original VGGT after fine-tuning on 3D object datasets, our approach achieves superior performance. This demonstrates the effectiveness of our generation-compatible framework in achieving accurate geometry and camera poses.

Table 3. **Quantitative Comparison of Depth Estimation.** Our method demonstrates superior accuracy in depth prediction compared to other baselines on both GSO and Toys4k datasets.

Method	GSO		Toys4k	
	Abs Rel ↓	RMSE ↓	Abs Rel ↓	RMSE ↓
VGGT [72]	0.0512	0.0686	0.0522	0.0735
ReconViaGen [2]	<u>0.0051</u>	<u>0.0081</u>	<u>0.0065</u>	<u>0.0109</u>
<b>Ours</b>	<b>0.0033</b>	<b>0.0057</b>	<b>0.0039</b>	<b>0.0075</b>

**Multi-view Consistent 3D Object Generation.** We evaluate our framework against a diverse set of state-of-the-art 3D reconstruction and generative models. Specifically, we compare against TRELIS-S [84], which utilizes a stochastic denoising process by randomly selecting a single input view for conditioning at each step, and TRELIS-M [84], which employs a multidiffusion approach to aggregate and average the denoised results from all available input views. We further include Hunyuan3D-MV [98], a multi-view Diffusion Transformer (DiT) designed for geometric synthesis, and LucidFusion [20], a feed-forward model based on Relative Coordinate Maps where we employ the LGM [64] framework for mesh extraction. For single-view foundations, we compare with SAM 3D [6]; given its single-image constraint, we report the best performance among four independent per-view runs. Finally, we compare with ReconViaGen [2], a concurrent baseline designed to unify sparse-view reconstruction with generative priors.

As shown in Table 1 and Fig. 5, our method consistently outperforms all baselines across both Toys4K and GSO datasets. Notably, LucidFusion exhibits a significant performance drop under our benchmark. This stems from its reliance on per-view geometry estimation, which is inherently unable to reconstruct unseen regions and struggles with unposed or perturbed camera translations in our evaluation. Furthermore, our framework demonstrates superior performance across all geometric metrics when compared to the concurrent work ReconViaGen. While ReconViaGen relies on injecting implicit features from a reconstruction branch into the generative process, our method provides explicit guidance by informing the generation model with intermediate reconstructed geometry. This strategy allows the model to better resolve spatial ambiguities and maintain stricter structural fidelity, suggesting that direct geometric conditioning is a more effective prior than high-level feature injection. These quantitative gains are further supported by the qualitative results in Fig. 5, demonstrating that our method outperforms other state-of-the-art baselines in both mesh quality and multi-view consistency. Our approach consistently delivers high-fidelity 3D object modeling results. As illustrated in Fig. 6, our model generalizes effectively to real-world sparse-view inputs, consistently achieving superior multi-view consistency and mesh quality. More qualitative results can be found in Fig. 7.

### 4.3 Ablation Studies

Due to the significant computational requirements of the full training cycle, we conduct our ablation studies on a reduced experimental scale. Specifically, we train the models using a subset of 2,000 objects sampled from our primary training set and evaluate performance on a held-out test set consisting of 50 diverse objects.

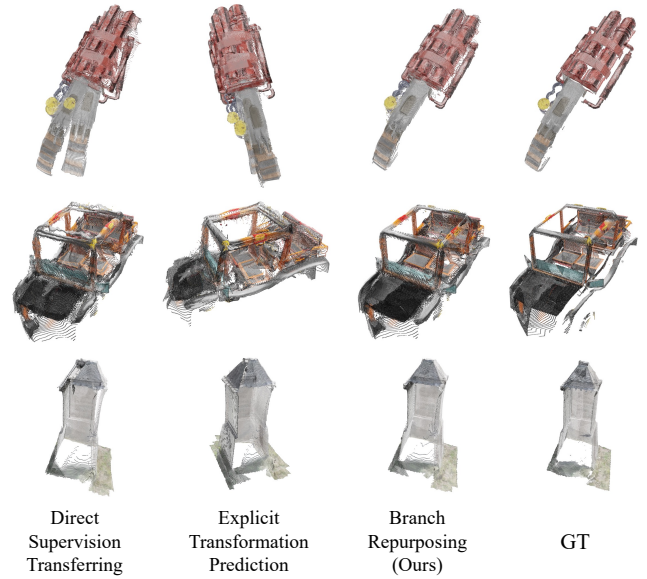


Fig. 3. **Qualitative Comparison of Canonical Alignment.** Our strategy achieves better geometric quality while aligning the canonical object space.

Table 4. **Quantitative Comparison of Canonical Alignment.** Compared with other strategies, our strategy is more accurate in camera pose prediction while remaining comparable in depth estimation.

Strategy	Camera Pose			Depth	
	ATE ↓	RPE <sub>t</sub> ↓	RPE <sub>r</sub> ↓	Abs Rel ↓	RMSE ↓
Direct Supervision Transferring	<u>0.2517</u>	<u>0.1414</u>	<u>4.2376</u>	0.0062	0.0210
Explicit Rigid Transformation	0.5934	0.1474	4.4596	<b>0.0049</b>	<b>0.0191</b>
<b>Branch Repurposing (Ours)</b>	<b>0.0353</b>	<b>0.0453</b>	<b>1.2181</b>	<u>0.0054</u>	<u>0.0200</u>

Table 5. **Quantitative Comparison of Multi-view Condition.** Our strategy achieves the best performance across most geometric metrics.

Strategy	Chamfer- $L_2$ ↓	Prec. ↑	Rec. ↑	F-Score ↑	Normal ↑	IoU ↑
Point-Guided Sampling	0.0260	0.7677	0.7087	0.7208	<b>0.8419</b>	0.6304
Latent-Augmented (Ours)	<b>0.0259</b>	<b>0.7890</b>	<b>0.7325</b>	<b>0.7428</b>	0.8350	<b>0.6707</b>

**Canonical Alignment Strategy.** A central challenge in our framework is reconciling the camera-centric reconstruction model with the canonical object space required by the diffusion generator. To address this, we compare our selective supervision strategy against two alternative approaches: explicit rigid transformation regression and direct supervision transferring. Quantitative and qualitative comparisons (Table 4 and Fig. 3) highlight the trade-offs of each method. While explicit regression achieves marginally better depth metrics, it suffers from the poorest global  $SE(3)$  alignment, as evidenced by a significantly higher ATE. This supports our hypothesis that regressing a global pose provides a weaker supervision signal for spatial alignment than dense, pointmap-based supervision. Conversely, direct supervision transferring leads to a marked performance decay in both camera pose and depth estimation. This suggests that enforcing a global coordinate shift without an adaptation mechanism disrupts the model’s pre-trained 3D priors. In contrast, our branch repurposing strategy achieves an optimal balance: it facilitates precise camera alignment and high-fidelity depth estimation by effectively canonicalizing the reference frame while preserving essential geometric priors.

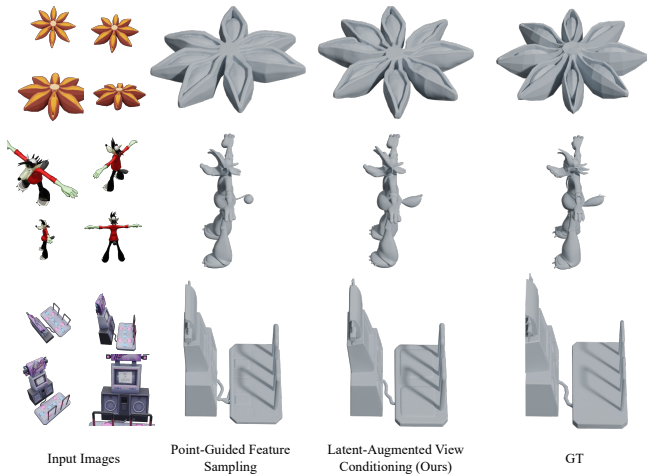


Fig. 4. **Qualitative Comparison of Multi-view Condition.** Our strategy (right) preserves dense image context more effectively than point-guided sampling (left), leading to improved input alignment.

**Multi-view Conditioning Strategy.** We evaluate our multi-view integration strategy by comparing our latent-augmented view conditioning against the point-guided sampling baseline introduced in Sec. 3.3. Quantitative results in Table 5 demonstrate that our approach leads to better 3D shape modeling performance. Qualitatively, Fig. 4 shows that the point-guided baseline can result in minor artifacts and inconsistencies. We attribute this to the fact that indexing image features with sparse points causes a loss of the original dense image context, which limits the model’s ability to maintain multi-view consistency. In contrast, our method preserves the complete dense feature set while augmenting it with geometric context.

#### 4.4 Conclusion

We present a unified framework that combines feed-forward multi-view reconstruction with controllable 3D diffusion to recover high-fidelity object geometry from unposed images. Our approach bridges the coordinate and representation gap between the two paradigms by canonicalizing reconstruction outputs and using them as explicit geometric guidance for multi-view conditioned generation. Extensive experiments show consistent improvements over strong reconstruction and generative baselines on Toys4K and GSO, and demonstrate robust generalization to real-world captures. By harmonizing these distinct methodologies, we aim to provide a foundation for the seamless unification of 3D reconstruction and generative modeling, fostering more integrated and versatile 3D vision systems. We plan to extend the framework to scene-level generation and incorporate texture synthesis.

#### References

- [1] Eric R Chan, Connor Z Lin, Matthew A Chan, Koki Nagano, Boxiao Pan, Shalini De Mello, Orazio Gallo, Leonidas Guibas, Jonathan Tremblay, Sameh Khamis, et al. 2022. Efficient geometry-aware 3D generative adversarial networks. In *IEEE/CVF International Conference on Computer Vision*.
- [2] Jiahao Chang, Chongjie Ye, Yushuang Wu, Yuantao Chen, Yidan Zhang, Zhongjin Luo, Chenghong Li, Yihao Zhi, and Xiaoguang Han. 2025. ReconViaGen: Towards Accurate Multi-view 3D Object Reconstruction via Generation. *arXiv preprint arXiv:2510.23306* (2025).
- [3] David Charatan, Sizhe Lester Li, Andrea Tagliasacchi, and Vincent Sitzmann. 2024. pixelSplat: 3d gaussian splats from image pairs for scalable generalizable 3d reconstruction. In *IEEE/CVF Conference on Computer Vision and Pattern Recognition*. 19457–19467.
- [4] Hansheng Chen, Jiatao Gu, Anpei Chen, Wei Tian, Zhuowen Tu, Lingjie Liu, and Hao Su. 2023. Single-stage diffusion nerf: A unified approach to 3d generation and reconstruction. In *Proceedings of the IEEE/CVF international conference on computer vision*. 2416–2425.
- [5] Sijin Chen, Xin Chen, Anqi Pang, Xianfang Zeng, Wei Cheng, Yijun Fu, Fukun Yin, Billz Wang, Jingyi Yu, Gang Yu, et al. 2024. Meshxl: Neural coordinate field for generative 3d foundation models. *Advances in Neural Information Processing Systems (NeurIPS)* (2024).
- [6] Xingyu Chen, Fu-Jen Chu, Pierre Gleize, Kevin J Liang, Alexander Sax, Hao Tang, Weiyao Wang, Michelle Guo, Thibaut Hardin, Xiang Li, et al. 2025. Sam 3d: 3dfy anything in images. *arXiv preprint arXiv:2511.16624* (2025).
- [7] Yiwen Chen, Tong He, Di Huang, Weicai Ye, Sijin Chen, Jiayang Tang, Xin Chen, Zhongang Cai, Lei Yang, Gang Yu, Guosheng Brand, and Chi Zhang. 2024. MeshAnything: Artist-Created Mesh Generation with Autoregressive Transformers. arXiv:2406.10163 [cs.CV] <https://arxiv.org/abs/2406.10163>
- [8] Yiwen Chen, Yikai Wang, Yihao Luo, Zhengyi Wang, Zilong Chen, Jun Zhu, Chi Zhang, and Guosheng Lin. 2024. MeshAnything V2: Artist-Created Mesh Generation With Adjacent Mesh Tokenization. arXiv:2408.02555 [cs.CV] <https://arxiv.org/abs/2408.02555>
- [9] Zilong Chen, Yikai Wang, Wenqiang Sun, Feng Wang, Yiwen Chen, and Huaping Liu. 2025. MeshGen: Generating PBR Textured Mesh with Render-Enhanced Auto-Encoder and Generative Data Augmentation. arXiv:2505.04656 [cs.GR] <https://arxiv.org/abs/2505.04656>
- [10] Zilong Chen, Yikai Wang, Feng Wang, Zhengyi Wang, and Huaping Liu. 2024. V3d: Video diffusion models are effective 3d generators. *arXiv preprint arXiv:2403.06738* (2024).
- [11] Matt Deitke, Ruoshi Liu, Matthew Wallingford, Huong Ngo, Oscar Michel, Aditya Kusupati, Alan Fan, Christian Laforte, Vikram Voleti, Samir Yitzhak Gadre, et al. 2023. Objaverse-xl: A universe of 10m+ 3d objects. *Advances in Neural Information Processing Systems* 36 (2023), 35799–35813.
- [12] Laura Downs, Anthony Francis, Nate Maggio, Brandon Cavalcanti, Gerard Tagliabue, Jake Varley, and Brian Ichter. 2022. Google scanned objects: A high-quality dataset of 3D scanned household items. In *2022 International Conference on Robotics and Automation (ICRA)*. IEEE, 2553–2560.
- [13] Zhiwen Fan, Wenyan Cong, Kairun Wen, Kevin Wang, Jian Zhang, Xinghao Ding, Danfei Xu, Boris Ivanovic, Marco Pavone, Georgios Pavlakos, et al. 2024. Instantsplat: Unbounded sparse-view pose-free gaussian splatting in 40 seconds. *arXiv preprint arXiv:2403.20309* 2, 3 (2024), 4.
- [14] Yang Fu, Sifei Liu, Amey Kulkarni, Jan Kautz, Alexei A Efros, and Xiaoqiang Wang. 2023. COLMAP-Free 3D Gaussian Splatting. *2024 IEEE/CVF Conference on Computer Vision and Pattern Recognition (CVPR)* (2023), 20796–20805.
- [15] Jun Gao, Tianchang Shen, Zian Wang, Wenzheng Chen, Kangxue Yin, Daiqing Li, Or Litany, Zan Gojcic, and Sanja Fidler. 2022. Get3d: A generative model of high quality 3d textured shapes learned from images. *Advances In Neural Information Processing Systems* 35 (2022), 31841–31854.
- [16] Hyojun Go, Dominik Narnhofer, Goutam Bhat, Prune Truong, Federico Tombari, and Konrad Schindler. 2025. VIST3A: Text-to-3D by Stitching a Multi-view Reconstruction Network to a Video Generator. *arXiv preprint arXiv:2510.13454* (2025).
- [17] Ian Goodfellow, Jean Pouget-Abadie, Mehdi Mirza, Bing Xu, David Warde-Farley, Sherjil Ozair, Aaron Courville, and Yoshua Bengio. 2014. Generative adversarial nets. *Advances in Neural Information Processing Systems* 27 (2014).
- [18] Xiaodong Gu, Zhiwen Fan, Siyu Zhu, Zuoqiuo Dai, Feitong Tan, and Ping Tan. 2020. Cascade Cost Volume for High-Resolution Multi-View Stereo and Stereo Matching. In *Proceedings of the IEEE/CVF Conference on Computer Vision and Pattern Recognition (CVPR)*. 2495–2504.
- [19] Zekun Hao, David W. Romero, Tsung-Yi Lin, and Ming-Yu Liu. 2024. Meshtron: High-Fidelity, Artist-Like 3D Mesh Generation at Scale. arXiv:2412.09548 [cs.GR] <https://arxiv.org/abs/2412.09548>
- [20] Hao He, Yixun Liang, Luozhou Wang, Yuanhao Cai, Xinli Xu, Hao-Xiang Guo, Xiang Wen, and Ying-Cong Chen. 2024. Lucidfusion: Generating 3d gaussians with arbitrary unposed images. (2024).
- [21] Xianglong He, Junyi Chen, Sida Peng, Di Huang, Yangguang Li, Xiaoshui Huang, Chun Yuan, Wanli Ouyang, and Tong He. 2024. GVGEN: Text-to-3D Generation with Volumetric Representation. In *European Conference on Computer Vision*.
- [22] Xianglong He, Zi-Xin Zou, Chia-Hao Chen, Yuan-Chen Guo, Ding Liang, Chun Yuan, Wanli Ouyang, Yan-Pei Cao, and Yangguang Li. 2025. SparseFlex: High-Resolution and Arbitrary-Topology 3D Shape Modeling. arXiv:2503.21732 [cs.CV] <https://arxiv.org/abs/2503.21732>
- [23] Jonathan Ho, Ajay Jain, and Pieter Abbeel. 2020. Denoising diffusion probabilistic models. *Advances in Neural Information Processing Systems* 33 (2020), 6840–6851.

- [24] Fangzhou Hong, Jiayang Tang, Ziang Cao, Min Shi, Tong Wu, Zhaoxi Chen, Tengfei Wang, Liang Pan, Dahua Lin, and Ziwei Liu. 2024. 3DTopia: Large Text-to-3D Generation Model with Hybrid Diffusion Priors. *CoRR* abs/2403.02234 (2024).
- [25] Jiaxin Huang, Yuanbo Yang, Bangbang Yang, Lin Ma, Yuewen Ma, and Yiyi Liao. 2026. Gen3R: 3D Scene Generation Meets Feed-Forward Reconstruction. *arXiv preprint arXiv:2601.04090* (2026).
- [26] Ka-Hei Hui, Ruihui Li, Jingyu Hu, and Chi-Wing Fu. 2022. Neural wavelet-domain diffusion for 3d shape generation. In *SIGGRAPH Asia 2022 Conference Papers*. 1–9.
- [27] Team Hunyuan3D, Shuhui Yang, Mingxin Yang, Yifei Feng, Xin Huang, Sheng Zhang, Zebin He, Di Luo, Haolin Liu, Yunfei Zhao, et al. 2025. Hunyuan3D 2.1: From Images to High-Fidelity 3D Assets with Production-Ready PBR Material. *arXiv preprint arXiv:2506.15442* (2025).
- [28] Team Hunyuan3D, Bowen Zhang, Chunchao Guo, Haolin Liu, Hongyu Yan, Huiwen Shi, Jingwei Huang, Junlin Yu, Kunhong Li, Penghao Wang, et al. 2025. Hunyuan3d-omni: A unified framework for controllable generation of 3d assets. *arXiv preprint arXiv:2509.21245* (2025).
- [29] Shubhendu Jena, Shishir Reddy Vutukur, and Adnan Boukhayma. 2025. SparSplat: Fast Multi-View Reconstruction with Generalizable 2D Gaussian Splatting. *arXiv preprint arXiv:2505.02175* (2025).
- [30] Bernhard Kerbl, Georgios Kopanas, Thomas Leimkühler, and George Drettakis. 2023. 3D Gaussian Splatting for Real-Time Radiance Field Rendering. *ACM Transactions on Graphics* 42, 4 (2023), 139–1.
- [31] Zeqiang Lai, Yunfei Zhao, Haolin Liu, Zibo Zhao, Qingxiang Lin, Huiwen Shi, Xianghui Yang, Mingxin Yang, Shuhui Yang, Yifei Feng, Sheng Zhang, Xin Huang, Di Luo, Fan Yang, Fang Yang, Lifu Wang, Sicong Liu, Yixuan Tang, Yulin Cai, Zebin He, Tian Liu, Yuhong Liu, Jie Jiang, Linus, Jingwei Huang, and Chunchao Guo. 2025. Hunyuan3D 2.5: Towards High-Fidelity 3D Assets Generation with Ultimate Details. *arXiv:2506.16504* [cs.CV] <https://arxiv.org/abs/2506.16504>
- [32] Yushi Lan, Fangzhou Hong, Shuai Yang, Shangchen Zhou, Xuyi Meng, Bo Dai, Xingang Pan, and Chen Change Loy. 2024. LN3Diff: Scalable Latent Neural Fields Diffusion for Speedy 3D Generation. In *ECCV*.
- [33] Vincent Leroy, Johann Cabon, and Jérôme Revaud. 2024. Grounding image matching in 3d with MAST3R. In *European Conference on Computer Vision*. 71–91.
- [34] Jiahao Li, Hao Tan, Kai Zhang, Zexiang Xu, Fujun Luan, Yinghao Xu, Yicong Hong, Kalyan Sunkavalli, Greg Shakhnarovich, and Sai Bi. 2023. Instant3d: Fast text-to-3d with sparse-view generation and large reconstruction model. *arXiv preprint arXiv:2311.06214* (2023).
- [35] Weiyu Li, Jiarui Liu, Rui Chen, Yixun Liang, Xuelin Chen, Ping Tan, and Xiaoxiao Long. 2024. CraftsMan: High-fidelity Mesh Generation with 3D Native Generation and Interactive Geometry Refiner. *arXiv preprint arXiv:2405.14979* (2024).
- [36] Yangguang Li, Zi-Xin Zou, Zexiang Liu, Dehu Wang, Yuan Liang, Zhipeng Yu, Xingchao Liu, Yuan-Chen Guo, Ding Liang, Wanli Ouyang, et al. 2025. TripoSG: High-Fidelity 3D Shape Synthesis using Large-Scale Rectified Flow Models. *arXiv preprint arXiv:2502.06608* (2025).
- [37] Zhihao Li, Yufei Wang, Heliang Zheng, Yihao Luo, and Bihan Wen. 2025. Sparc3D: Sparse Representation and Construction for High-Resolution 3D Shapes Modeling. *arXiv:2505.14521* [cs.CV] <https://arxiv.org/abs/2505.14521>
- [38] Hanwen Liang, Junli Cao, Vidit Goel, Guocheng Qian, Sergei Korolev, Demetri Terzopoulos, Konstantinos N Plataniotis, Sergey Tulyakov, and Jian Ren. 2025. Wonderland: Navigating 3d scenes from a single image. In *IEEE/CVF Conference on Computer Vision and Pattern Recognition*. 798–810.
- [39] Chenguo Lin, Panwang Pan, Bangbang Yang, Zeming Li, and Yadong MU. 2025. DiffSplat: Repurposing Image Diffusion Models for Scalable Gaussian Splat Generation. In *International Conference on Learning Representations*.
- [40] Chen-Hsuan Lin, Wei-Chiu Ma, Antonio Torralba, and Simon Lucey. 2021. BARF: Bundle-Adjusting Neural Radiance Fields. In *Proceedings of the IEEE/CVF International Conference on Computer Vision (ICCV)*. 5741–5751.
- [41] Yuchen Lin, Chenguo Lin, Panwang Pan, Honglei Yan, Yiqiang Feng, Yadong Mu, and Katerina Fragkiadaki. 2025. PartCrafter: Structured 3D Mesh Generation via Compositional Latent Diffusion Transformers. *arXiv:2506.05573* [cs.CV] <https://arxiv.org/abs/2506.05573>
- [42] Minghua Liu, Chao Xu, Haian Jin, Linghao Chen, Mukund Varma T, Zexiang Xu, and Hao Su. 2023. One-2-3-45: Any single image to 3d mesh in 45 seconds without per-shape optimization. *Advances in Neural Information Processing Systems* 36 (2023), 22226–22246.
- [43] Ruoshi Liu, Rundui Wu, Basile Van Hoorick, Pavel Tokmakov, Sergey Zakharov, and Carl Vondrick. 2023. Zero-1-to-3: Zero-shot one image to 3d object. In *Proceedings of the IEEE/CVF international conference on computer vision*. 9298–9309.
- [44] Xiaoxiao Long, Yuan-Chen Guo, Cheng Lin, Yuan Liu, Zhiyang Dou, Lingjie Liu, Yuexin Ma, Song-Hai Zhang, Marc Habermann, Christian Theobalt, et al. 2024. Wonder3d: Single image to 3d using cross-domain diffusion. In *Proceedings of the IEEE/CVF Conference on Computer Vision and Pattern Recognition*. 9970–9980.
- [45] William E Lorensen and Harvey E Cline. 1987. Marching cubes: A high resolution 3D surface construction algorithm. *ACM SIGGRAPH Computer Graphics* 21, 4 (1987), 163–169.
- [46] Shitong Luo and Wei Hu. 2021. Diffusion probabilistic models for 3d point cloud generation. In *Proceedings of the IEEE/CVF conference on computer vision and pattern recognition*. 2837–2845.
- [47] Ben Mildenhall, Pratul P Srinivasan, Matthew Tancik, Jonathan T Barron, Ravi Ramamoorthi, and Ren Ng. 2020. NeRF: Representing Scenes as Neural Radiance Fields for View Synthesis. In *European Conference on Computer Vision (ECCV)*. 405–421.
- [48] Norman Müller, Yawar Siddiqui, Lorenzo Porzi, Samuel Rota Bulo, Peter Kotschieder, and Matthias Nießner. 2023. DiffRF: Rendering-guided 3d radiance field diffusion. In *Proceedings of the IEEE/CVF Conference on Computer Vision and Pattern Recognition*. 4328–4338.
- [49] Alex Nichol, Heewoo Jun, Prafulla Dhariwal, Pamela Mishkin, and Mark Chen. 2022. Point-e: A system for generating 3d point clouds from complex prompts. *arXiv preprint arXiv:2212.08751* (2022).
- [50] Michael Niemeyer, Jonathan T. Barron, Ben Mildenhall, Mehdi S. M. Sajjadi, Andreas Geiger, and Noha Radwan. 2022. RegNeRF: Regularizing Neural Radiance Fields for View Synthesis from Sparse Inputs. In *2022 IEEE/CVF Conference on Computer Vision and Pattern Recognition (CVPR)*. IEEE, New Orleans, LA, USA. doi:10.1109/CVPR52688.2022.00540
- [51] Maxime Oquab, Timothée Darcet, Théo Moutakanni, Huy Vo, Marc Szafraniec, Vasil Khalidov, Pierre Fernandez, Daniel Haziza, Francisco Massa, Alaaeldin El-Nouby, et al. 2023. Dinov2: Learning robust visual features without supervision. *arXiv preprint arXiv:2304.07193* (2023).
- [52] Jeong Joon Park, Peter Florence, Julian Straub, Richard Newcombe, and Steven Lovegrove. 2019. Deepsdf: Learning continuous signed distance functions for shape representation. In *Proceedings of the IEEE/CVF conference on computer vision and pattern recognition*. 165–174.
- [53] Ben Poole, Ajay Jain, Jonathan T Barron, and Ben Mildenhall. 2023. DreamFusion: Text-to-3D using 2D Diffusion. In *International Conference on Learning Representations*.
- [54] Robin Rombach, Andreas Blattmann, Dominik Lorenz, Patrick Esser, and Björn Ommer. 2022. High-resolution image synthesis with latent diffusion models. In *Proceedings of the IEEE/CVF Conference on Computer Vision and Pattern Recognition*. 10684–10695.
- [55] Johannes L Schönberger and Jan-Michael Frahm. 2016. Structure-from-motion revisited. In *IEEE Conference on Computer Vision and Pattern Recognition*. 4104–4113.
- [56] Johannes L. Schönberger, Enliang Zheng, Marc Pollefeys, and Jan-Michael Frahm. 2016. Pixelwise View Selection for Unstructured Multi-View Stereo. In *European Conference on Computer Vision (ECCV)*. 501–518.
- [57] Katja Schwarz, Norman Mueller, and Peter Kotschieder. 2025. Generative Gaussian splatting: Generating 3D scenes with video diffusion priors. *arXiv preprint arXiv:2503.13272* (2025).
- [58] Yichun Shi, Peng Wang, Jianglong Ye, Long Mai, Kejie Li, and Xiao Yang. 2024. MVDream: Multi-view Diffusion for 3D Generation. In *International Conference on Learning Representations*.
- [59] Yawar Siddiqui, Antonio Alliegro, Alexey Artemov, Tatiana Tommasi, Daniele Sirigatti, Vladislav Rosov, Angela Dai, and Matthias Nießner. 2024. Meshgpt: Generating triangle meshes with decoder-only transformers. In *Proceedings of the IEEE/CVF Conference on Computer Vision and Pattern Recognition (CVPR)*.
- [60] Jascha Sohl-Dickstein, Eric Weiss, Niru Maheswaranathan, and Surya Ganguli. 2015. Deep unsupervised learning using nonequilibrium thermodynamics. In *International Conference on Machine Learning*. 2256–2265.
- [61] Stefan Stojanov, Anh Thai, and James M Rehg. 2021. Using shape to categorize: Low-shot learning with an explicit shape bias. In *Proceedings of the IEEE/CVF conference on computer vision and pattern recognition*. 1798–1808.
- [62] Stanislaw Szymonowicz, Jason Y Zhang, Pratul Srinivasan, Ruiqi Gao, Arthur Brussee, Aleksander Holynski, Ricardo Martin-Brualla, Jonathan T Barron, and Philipp Henzler. 2025. Bolt3D: Generating 3D scenes in seconds. *arXiv preprint arXiv:2503.14445* (2025).
- [63] Bin Tan, Nan Xue, Tianfu Wu, and Gui-Song Xia. 2023. NOPE-SAC: Neural One-Plane RANSAC for Sparse-View Planar 3D Reconstruction. *IEEE Transactions on Pattern Analysis and Machine Intelligence* 45 (2023). doi:10.1109/TPAMI.2023.3314745
- [64] Jiayang Tang, Zhaoxi Chen, Xiaokang Chen, Tengfei Wang, Gang Zeng, and Ziwei Liu. 2024. Lgm: Large multi-view gaussian model for high-resolution 3d content creation. In *European Conference on Computer Vision*. 1–18.
- [65] Jiayang Tang, Zhaoshuo Li, Zekun Hao, Xian Liu, Gang Zeng, Ming-Yu Liu, and Qingsheng Zhang. 2024. EdgeRunner: Auto-regressive Auto-encoder for Artistic Mesh Generation. *arXiv:2409.18114* [cs.CV] <https://arxiv.org/abs/2409.18114>
- [66] Jiayang Tang, Ruijie Lu, Zhaoshuo Li, Zekun Hao, Xuan Li, Fangyin Wei, Shuran Song, Gang Zeng, Ming-Yu Liu, and Tsung-Yi Lin. 2025. Efficient Part-level

- 3D Object Generation via Dual Volume Packing. arXiv:2506.09980 [cs.CV] <https://arxiv.org/abs/2506.09980>
- [67] Junshu Tang, Tengfei Wang, Bo Zhang, Ting Zhang, Ran Yi, Lizhuang Ma, and Dong Chen. 2023. Make-it-3d: High-fidelity 3d creation from a single image with diffusion prior. In *Proceedings of the IEEE/CVF international conference on computer vision*. 22819–22829.
- [68] Shengji Tang, Weicai Ye, Peng Ye, Weihao Lin, Yang Zhou, Tao Chen, and Wanli Ouyang. 2024. HiSplat: Hierarchical 3D Gaussian Splatting for Generalizable Sparse-View Reconstruction. *arXiv preprint arXiv:2410.06245* (2024).
- [69] Arash Vahdat, Francis Williams, Zan Gojcic, Or Litany, Sanja Fidler, Karsten Kreis, et al. 2022. Lion: Latent point diffusion models for 3d shape generation. *Advances in Neural Information Processing Systems* 35 (2022), 10021–10039.
- [70] Vikram Voleti, Chun-Han Yao, Mark Boss, Adam Letts, David Pankratz, Dmitry Tochilkin, Christian Laforte, Robin Rombach, and Varun Jampani. 2024. Sv3d: Novel multi-view synthesis and 3d generation from a single image using latent video diffusion. In *European Conference on Computer Vision*. Springer, 439–457.
- [71] Fangjinhua Wang, Silvano Galliani, Christoph Vogel, Pablo Speciale, and Marc Pollefeys. 2021. PatchmatchNet: Learned Multi-View Patchmatch Stereo. In *Proceedings of the IEEE/CVF Conference on Computer Vision and Pattern Recognition (CVPR)*. 14194–14203.
- [72] Jianyuan Wang, Minghao Chen, Nikita Karaev, Andrea Vedaldi, Christian Rupprecht, and David Novotny. 2025. VGGT: Visual geometry grounded transformer. In *IEEE/CVF Conference on Computer Vision and Pattern Recognition*. 5294–5306.
- [73] Peng Wang, Hao Tan, Sai Bi, Yinghao Xu, Fujun Luan, Kalyan Sunkavalli, Wenping Wang, Zexiang Xu, and Kai Zhang. 2024. PF-LRM: Pose-Free Large Reconstruction Model for Joint Pose and Shape Prediction. In *ICLR*.
- [74] Qianqian Wang, Zhicheng Wang, Kyle Genova, Pratul P Srinivasan, Howard Zhou, Jonathan T Barron, Ricardo Martin-Brualla, Noah Snavely, and Thomas Funkhouser. 2021. Ibrnet: Learning multi-view image-based rendering. In *Proceedings of the IEEE/CVF conference on computer vision and pattern recognition*. 4690–4699.
- [75] Shuzhe Wang, Vincent Leroy, Yohann Cabon, Boris Chidlovskii, and Jerome Revaud. 2024. DUST3R: Geometric 3D Vision Made Easy. In *Proceedings of the IEEE/CVF Conference on Computer Vision and Pattern Recognition (CVPR)*. 20697–20709.
- [76] Yifan Wang, Jianjun Zhou, Haoyi Zhu, Wenzheng Chang, Yang Zhou, Zizun Li, Junyi Chen, Jiangmiao Pang, Chunhua Shen, and Tong He. 2025.  $\pi$ 3: Scalable Permutation-Equivariant Visual Geometry Learning. *arXiv preprint arXiv:2507.13347* (2025).
- [77] Zhengyi Wang, Jonathan Lorraine, Yikai Wang, Hang Su, Jun Zhu, Sanja Fidler, and Xiaohui Zeng. 2024. LLaMA-Mesh: Unifying 3D Mesh Generation with Language Models. arXiv:2411.09595 [cs.LG] <https://arxiv.org/abs/2411.09595>
- [78] Zhengyi Wang, Cheng Lu, Yikai Wang, Fan Bao, Chongxuan Li, Hang Su, and Jun Zhu. 2023. ProlificDreamer: high-fidelity and diverse text-to-3D generation with variational score distillation. *Advances in Neural Information Processing Systems* 36 (2023), 8406–8441.
- [79] Haohan Weng, Zibo Zhao, Biwen Lei, Xianghui Yang, Jian Liu, Zeqiang Lai, Zhuo Chen, Yuhong Liu, Jie Jiang, Chunchao Guo, Tong Zhang, Shenghua Gao, and C. L. Philip Chen. 2024. Scaling Mesh Generation via Compressive Tokenization. arXiv:2411.07025 [cs.GR] <https://arxiv.org/abs/2411.07025>
- [80] Jiajun Wu, Chengkai Zhang, Tianfan Xue, Bill Freeman, and Josh Tenenbaum. 2016. Learning a probabilistic latent space of object shapes via 3d generative-adversarial modeling. *Advances in neural information processing systems* 29 (2016).
- [81] Rundi Wu, Ben Mildenhall, Philipp Henzler, Keunhong Park, Ruiqi Gao, Daniel Watson, Pratul P Srinivasan, Dor Verbin, Jonathan T Barron, Ben Poole, et al. 2024. Reconfusion: 3d reconstruction with diffusion priors. In *Proceedings of the IEEE/CVF conference on computer vision and pattern recognition*. 21551–21561.
- [82] Shuang Wu, Youtian Lin, Feihu Zhang, Yifei Zeng, Jingxi Xu, Philip Torr, Xun Cao, and Yao Yao. 2024. Direct3D: Scalable Image-to-3D Generation via 3D Latent Diffusion Transformer. *Advances in Neural Information Processing Systems* 37 (2024), 121859–121881.
- [83] Shuang Wu, Youtian Lin, Feihu Zhang, Yifei Zeng, Yikang Yang, Yajie Bao, Jiachen Qian, Siyu Zhu, Xun Cao, Philip Torr, and Yao Yao. 2025. Direct3D-S2: Gigascale 3D Generation Made Easy with Spatial Sparse Attention. arXiv:2505.17412 [cs.CV] <https://arxiv.org/abs/2505.17412>
- [84] Jianfeng Xiang, Zelong Lv, Sicheng Xu, Yu Deng, Ruicheng Wang, Bowen Zhang, Dong Chen, Xin Tong, and Jiaolong Yang. 2025. Structured 3D Latents for Scalable and Versatile 3D Generation. arXiv:2412.01506 [cs.CV] <https://arxiv.org/abs/2412.01506>
- [85] Jiale Xu, Weihao Cheng, Yiming Gao, Xintao Wang, Shenghua Gao, and Ying Shan. 2024. Instantmesh: Efficient 3d mesh generation from a single image with sparse-view large reconstruction models. *arXiv preprint arXiv:2404.07191* (2024).
- [86] Jianing Yang, Alexander Sax, Kevin J Liang, Mikael Henaff, Hao Tang, Ang Cao, Joyce Chai, Franziska Meier, and Matt Feiszli. 2025. Fast3R: Towards 3d reconstruction of 1000+ images in one forward pass. In *IEEE/CVF Conference on Computer Vision and Pattern Recognition*. 21924–21935.
- [87] Yunhan Yang, Yuan-Chen Guo, Yukun Huang, Zi-Xin Zou, Zhipeng Yu, Yangguang Li, Yan-Pei Cao, and Xihui Liu. 2025. HoloPart: Generative 3D Part Amodal Segmentation. arXiv:2504.07943 [cs.CV] <https://arxiv.org/abs/2504.07943>
- [88] Yuanbo Yang, Jiahao Shao, Xinyang Li, Yujun Shen, Andreas Geiger, and Yiyi Liao. 2025. Prometheus: 3d-aware latent diffusion models for feed-forward text-to-3d scene generation. In *IEEE/CVF Conference on Computer Vision and Pattern Recognition*. 2857–2869.
- [89] Yao Yao, Zixin Luo, Shiwei Li, Tian Fang, and Long Quan. 2018. MVSNet: Depth Inference for Unstructured Multi-view Stereo. In *European Conference on Computer Vision (ECCV)*. 767–783.
- [90] Yao Yao, Zixin Luo, Shiwei Li, Tianwei Shen, Tian Fang, and Long Quan. 2019. Recurrent MVSNet for High-resolution Multi-view Stereo Depth Inference. In *Proceedings of the IEEE/CVF Conference on Computer Vision and Pattern Recognition (CVPR)*. 5525–5534.
- [91] Chongjie Ye, Yushuang Wu, Ziteng Lu, Jiahao Chang, Xiaoyang Guo, Jiaqing Zhou, Hao Zhao, and Xiaoguang Han. 2025. Hi3DGen: High-fidelity 3D Geometry Generation from Images via Normal Bridging. *arXiv preprint arXiv:2503.22236* (2025).
- [92] Alex Yu, Vickie Ye, Matthew Tancik, and Angjoo Kanazawa. 2021. pixelNeRF: Neural Radiance Fields from One or Few Images. In *Proceedings of the IEEE/CVF Conference on Computer Vision and Pattern Recognition (CVPR)*. 4576–4585. doi:10.1109/CVPR46437.2021.00455
- [93] Bowen Zhang, Yiji Cheng, Jiaolong Yang, Chunyu Wang, Feng Zhao, Yansong Tang, Dong Chen, and Baining Guo. 2024. GaussianCube: Structuring Gaussian Splatting using Optimal Transport for 3D Generative Modeling. *arXiv preprint arXiv:2403.19655* (2024).
- [94] Biao Zhang, Jiapeng Tang, Matthias Niessner, and Peter Wonka. 2023. 3dshape2vecset: A 3d shape representation for neural fields and generative diffusion models. *ACM Transactions on Graphics* 42, 4 (2023), 1–16.
- [95] Chuanrui Zhang, Yingshuang Zou, Zhuoling Li, Minmin Yi, and Haoqian Wang. 2025. Transplat: Generalizable 3d gaussian splatting from sparse multi-view images with transformers. In *Proceedings of the AAAI Conference on Artificial Intelligence*, Vol. 39. 9869–9877.
- [96] Longwen Zhang, Ziyu Wang, Qixuan Zhang, Qiwei Qiu, Anqi Pang, Haoran Jiang, Wei Yang, Lan Xu, and Jingyi Yu. 2024. CLAY: A Controllable Large-scale Generative Model for Creating High-quality 3D Assets. *ACM Transactions on Graphics* 43, 4 (2024), 1–20.
- [97] Ruowen Zhao, Junliang Ye, Zhengyi Wang, Guangce Liu, Yiwen Chen, Yikai Wang, and Jun Zhu. 2025. DeepMesh: Auto-Regressive Artist-mesh Creation with Reinforcement Learning. arXiv:2503.15265 [cs.CV] <https://arxiv.org/abs/2503.15265>
- [98] Zibo Zhao, Zeqiang Lai, Qingxiang Lin, Yunfei Zhao, Haolin Liu, Shuhui Yang, Yifei Feng, Mingxin Yang, Sheng Zhang, Xianghui Yang, Huiwen Shi, Sicong Liu, Junta Wu, Yihang Lian, Fan Yang, Ruining Tang, Zebin He, Xinzhou Wang, Jian Liu, Xuhui Zuo, Zhuo Chen, Biwen Lei, Haohan Weng, Jing Xu, Yiling Zhu, Xinhai Liu, Lixin Xu, Changrong Hu, Shaoxiang Yang, Song Zhang, Yang Liu, Tianyu Huang, Lifu Wang, Jihong Zhang, Meng Chen, Liang Dong, Yiwen Jia, Yulin Cai, Jiaao Yu, Yixuan Tang, Hao Zhang, Zheng Ye, Peng He, Runzhou Wu, Chao Zhang, Yonghao Tan, Jie Xiao, Yangyu Tao, Jianchen Zhu, Jinbao Xue, Kai Liu, Chongqing Zhao, Ximeng Wu, Zhichao Hu, Lei Qin, Jianbing Peng, Zhan Li, Minghui Chen, Xipeng Zhang, Lin Niu, Paige Wang, Yingkai Wang, Haozhao Kuang, Zhongyi Fan, Xu Zheng, and Weihao Zh.. 2025. Hunyuan3D 2.0: Scaling Diffusion Models for High Resolution Textured 3D Assets Generation. arXiv:2501.12202 [cs.CV] <https://arxiv.org/abs/2501.12202>
- [99] Zibo Zhao, Wen Liu, Xin Chen, Xianfang Zeng, Rui Wang, Pei Cheng, Bin Fu, Tao Chen, Gang Yu, and Shenghua Gao. 2023. Michelangelo: Conditional 3d shape generation based on shape-image-text aligned latent representation. *Advances in Neural Information Processing Systems* 36 (2023), 73969–73982.
- [100] Xinyang Zheng, Yang Liu, Pengshuai Wang, and Xin Tong. 2022. SDF-StyleGAN: Implicit SDF-Based StyleGAN for 3D Shape Generation. In *Computer Graphics Forum*, Vol. 41. 52–63.

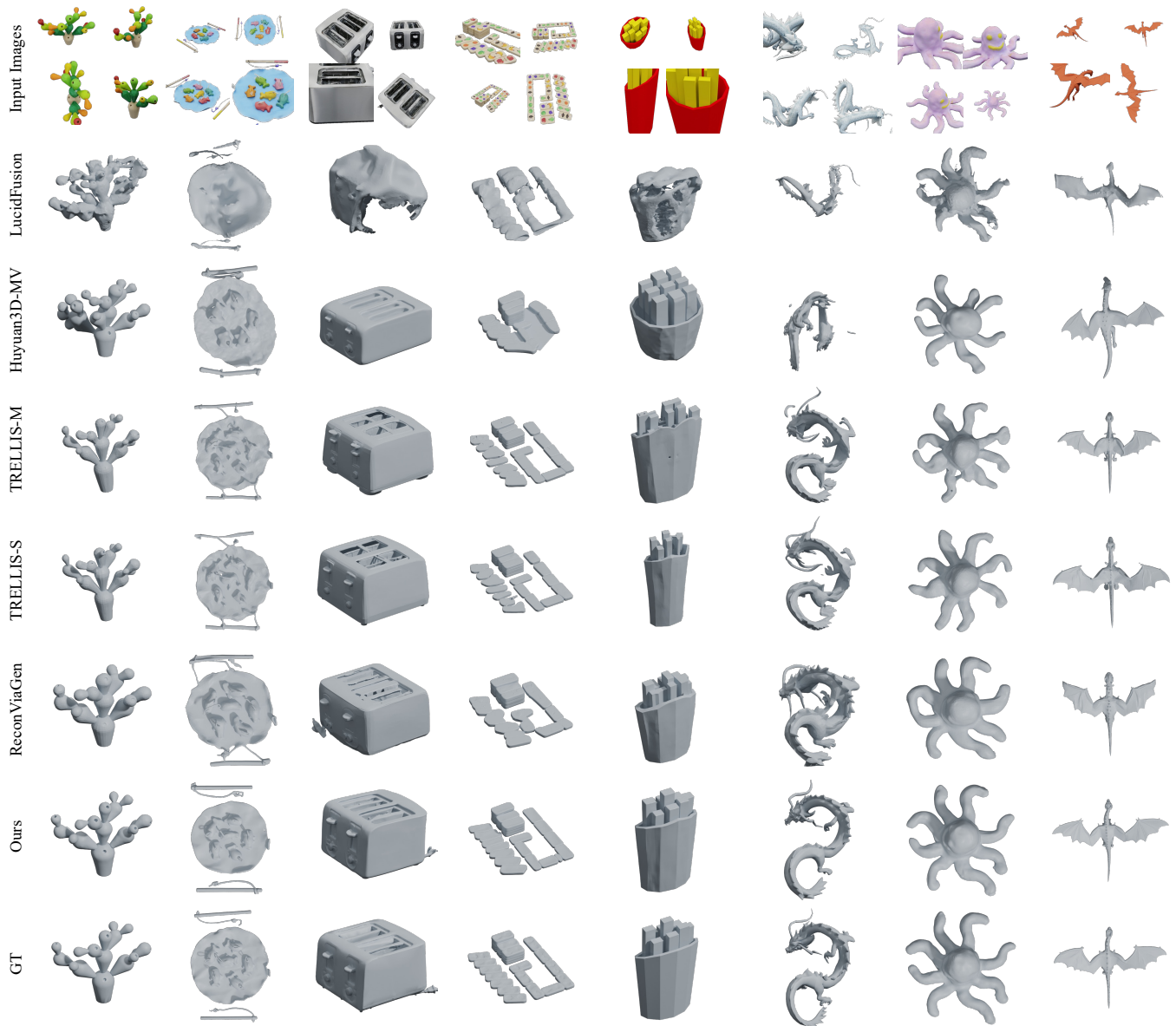


Fig. 5. **Qualitative Comparison on Toys4K and GSO.** Compared to state-of-the-art reconstruction and generative baselines, our method produces 3D meshes with higher structural fidelity and superior multi-view consistency from sparse inputs.

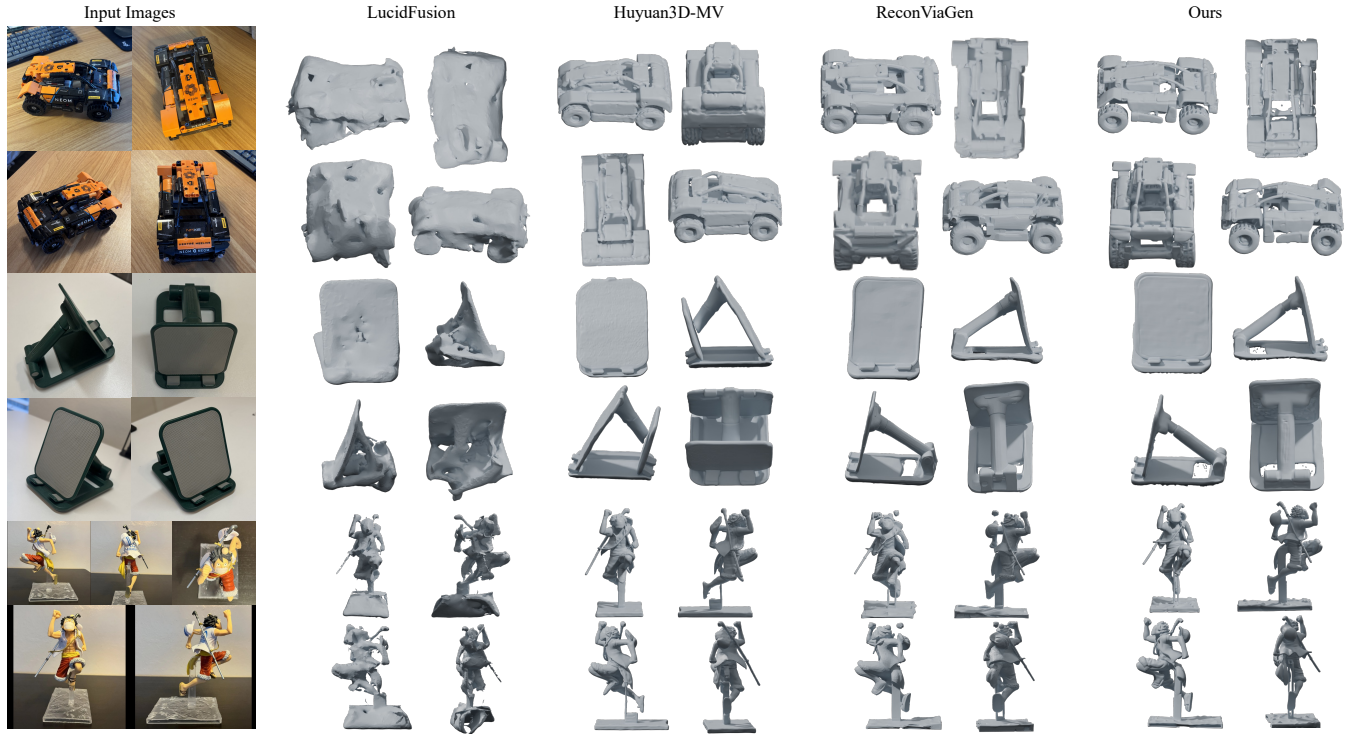


Fig. 6. **Generalization to Real-world Environments.** Our framework demonstrates robustness and superior performance compared to SOTA method.

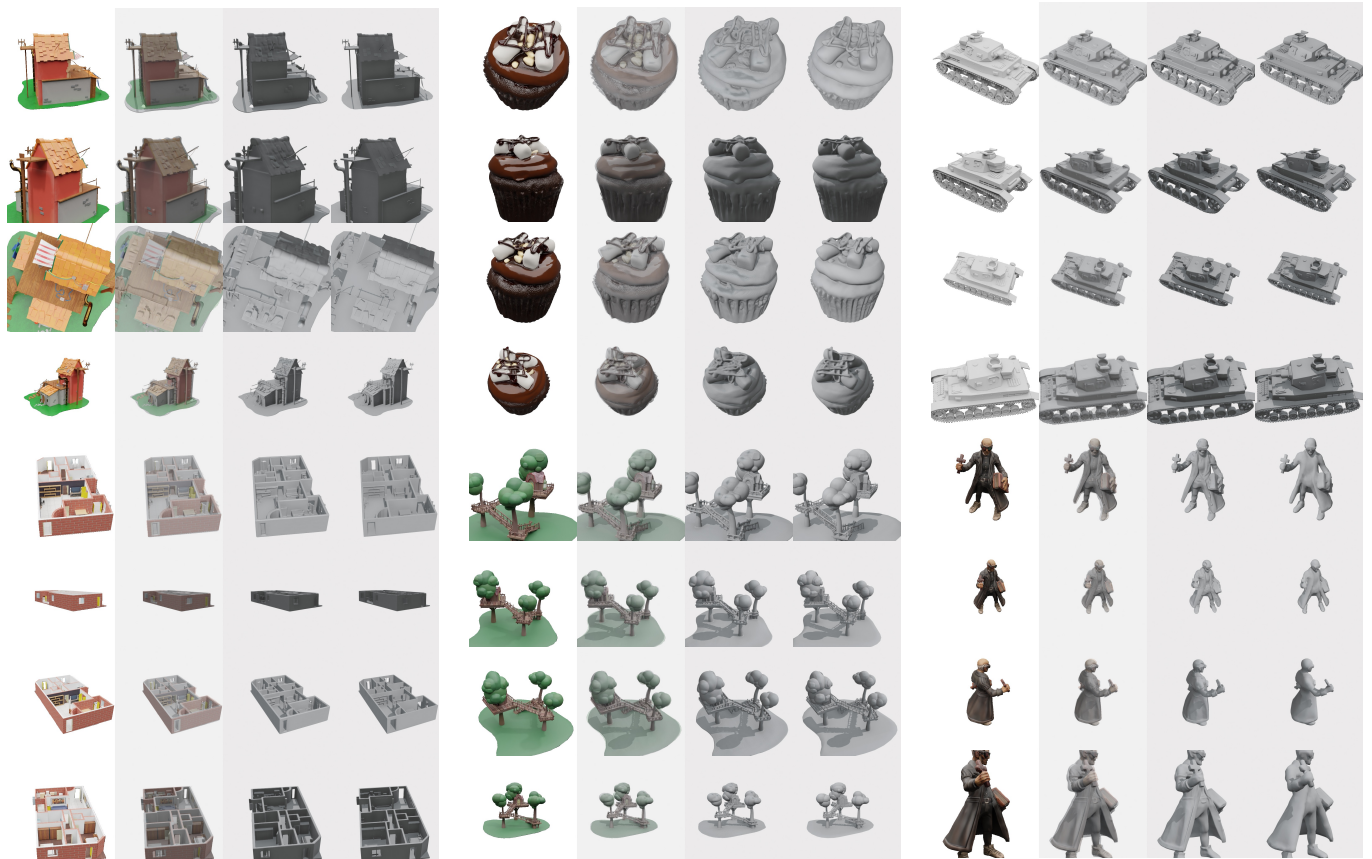


Fig. 7. **Additional qualitative results.** We show six multi-view shape modeling examples. For each of four input views, from left to right we show: the input image, our mesh rendering overlaid on the input image, our mesh rendering, and the ground-truth mesh rendering.